Instability Growth Patterns of a Shock-Accelerated Thin Fluid Layer

J. W. Jacobs
Department of Aerospace and Mechanical Engineering, University of Arizona, Tucson, Arizona 85721

D. L. Klein,[a] D. G. Jenkins,[b] and R. F. Benjamin
Los Alamos National Laboratory, Los Alamos, New Mexico 87545
(Received 13 October 1992)

Laser-induced fluorescence imaging of a shock-accelerated thin gas layer, produced by a planar SF_6 jet in air, shows multiple flow evolutions. Richtmyer-Meshkov instability causes spatially periodic perturbations initially imposed on the jet to develop into one of three distinct flow patterns, indicating nonlinear instability growth. Slight differences in the vorticity distribution deposited on the air-SF_6 interfaces by the shock interaction produce a bifurcated flow, observed as mushroom-shaped or sinuous-shaped interfacial patterns.

PACS numbers: 47.40.Nm, 47.20.Ky, 47.55.−t

A fundamental problem in fluid mechanics is the stability of an interface between fluids of different densities. Interfacial instabilities include the Rayleigh-Taylor (RT) instability for a constantly accelerated interface and the Richtmyer-Meshkov (RM) [1–3] instability for an impulsively accelerated interface. The RT instability occurs when density and pressure gradients are opposed. By contrast, the RM instability occurs when density and pressure gradients are either opposed or aligned. The fluid flows induced by these instabilities are of practical interest in applications as diverse as climate modeling, convection within planetary interiors, astrophysics, and inertial confinement fusion. Early stages of these instabilities are well characterized by linear perturbation theory, and later stages evolve into turbulence. Little is known about the intermediate, "nonlinear" stage of the RM instability.

We have studied the evolution of a shock-accelerated thin fluid layer, for which the interfaces on both sides of the layer are RM unstable. For initial conditions which are indistinguishable by measurement techniques available for our work, we observe that the intermediate growth stage of this flow evolves into one of three distinct sets of patterns during each experiment. We are unable to control or predict which pattern emerges on each experiment. To our knowledge, these are the first observations of a shock-driven instability with this characteristic of bifurcating flows. We suggest that these flow evolutions can be attributed to interactions among shock-induced vorticity distributions, and that they are extremely sensitive to initial conditions. The observed, preturbulent flows are transient states, persisting about 1 ms in these experiments.

Our experimental technique uses PLIF (planar laser-induced fluorescence) imaging of the cross section of a thin gas layer created by a curtain of vertically flowing SF_6 within a shock tube. The cross section of the layer has a varicose profile, designed to impose perturbations on both upstream and downstream interfaces. The PLIF imaging technique was used by Jacobs [4] to visualize the flow of shock-accelerated cylindrical jets. The test section shown schematically in Fig. 1 shows the perturbed SF_6 layer being shock accelerated by the Mach 1.2 shock wave, corresponding to a shock wave speed of 0.41 km/s. A spatially modulated planar SF_6 jet from a contoured nozzle forms the perturbed gas layer (i.e., the gas curtain) without use of a membrane. Membranes used in previous experiments [2,3] modified and obscured the flow. An outlet slot placed opposite the inlet at the bottom of the viewing section removes the SF_6 along with some makeup air to prevent SF_6 contamination of the shock tube. The makeup air enters the shock tube far upstream and downstream of the viewing section to minimize the disruptive effects at the air/SF_6 interfaces.

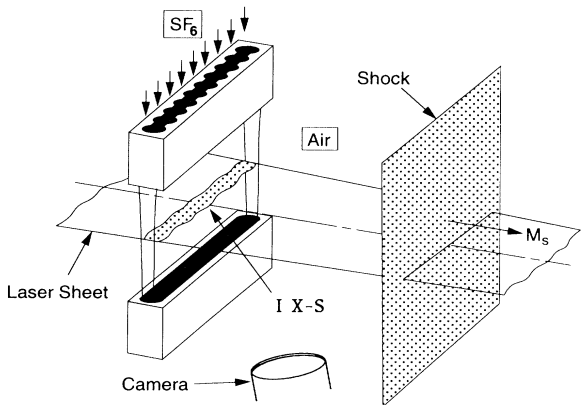

FIG. 1. The perturbed, thin layer of SF_6/diacetyl flows downward in the shock-tube test section from a plenum-nozzle assembly atop, through the test section, and into an exhaust vent below. The PLIF probe is a horizontal laser sheet that intersects the thin layer at the illuminated cross section, denoted IX-S, which the intensified CCD camera views. The incident shock accelerates the layer from left to right, and the observed profiles are displaced downstream from the initial position depicted in this diagram. The profile of the flow seen in the IX-S region is smoothed relative to the nozzle profile, but the dominant perturbation wavelength remains the same.

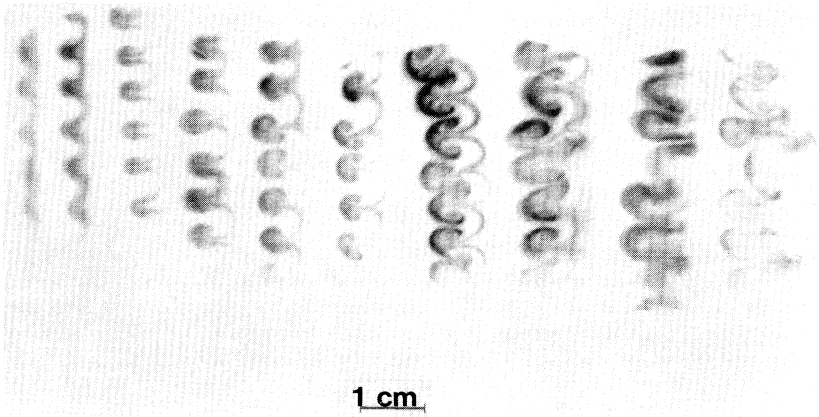

FIG. 2. This time sequence of PLIF images shows clearly one of the three distinct profiles that evolve from nearly identical initial conditions. Interframe time is about 100 μs. Because each image is taken on a different event, detailed features do not register frame to frame. However, the dominant growth features are reproducible. These "upstream mushrooms" have the mushroom caps oriented opposite to the direction of shock-wave motion. Darker regions indicate stronger fluorescent emission and therefore higher concentration of SF_6/diacetyl.

PLIF flow visualization uses a horizontal planar sheet of 440-nm wavelength light from a flashlamp-pumped dye laser to illuminate the SF_6 layer seeded with a fluorescent tracer, diacetyl vapor [5], which stays mixed with SF_6 because molecular masses are close. The 10-μs duration laser pulse enables only one image per event, so we are unable to observe both initial conditions and a dynamic image on the same event. A gated, intensified charge-coupled-device (CCD) camera records the fluorescent image, which is a cross section of the SF_6 flow, assuming the fluorescent signal is proportional to SF_6 density. Long-pass optical filters block the incident laser light.

Figures 2, 3, and 4 show sequences of fluorescent images depicting the three reproducible and distinct flow patterns that evolve from shock accelerating the initially perturbed layer. Each image is taken on a different experiment. In Fig. 2 the perturbed layer forms a series of vortex pairs, observed as "mushrooms," which are oriented opposite to the shock direction, i.e., the mushroom caps are on the upstream side of the moving interface. In Fig. 3, the flow forms vortex pairs (i.e., mushrooms) oriented downstream. Figure 4 shows the development of a sinuous profile. The three instability modes occur randomly with upstream mushrooms appearing about 40% of the time, downstream mushrooms 10% of the time, and sinuous profile 50% of the time. We did not observe upstream and downstream mushrooms in the same image except at late times when interaction among neighboring mushrooms occurs.

The three modes of instability evolve from nearly identical initial conditions. PLIF images of the initial cross section taken at 250-ms intervals (the minimum inter-

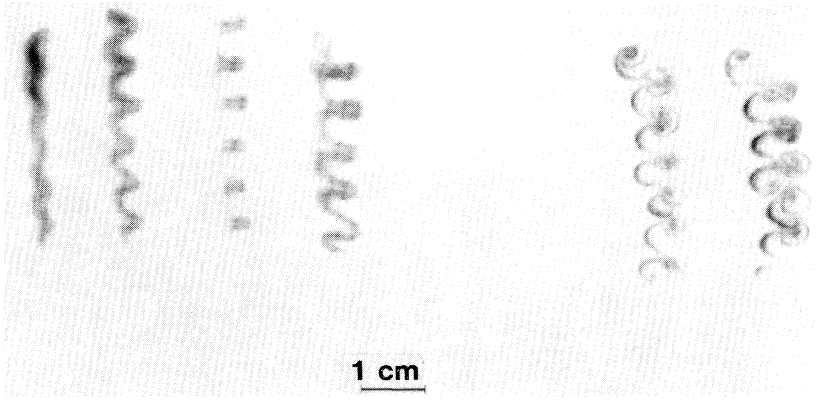

FIG. 3. The "downstream mushrooms" are similar to the upstream mushrooms but oppositely directed. They occur rarely in our experiments. Like upstream mushrooms, they appear to be driven by vortex pairs and produce mixing by entraining the ambient air within the SF_6 test gas.

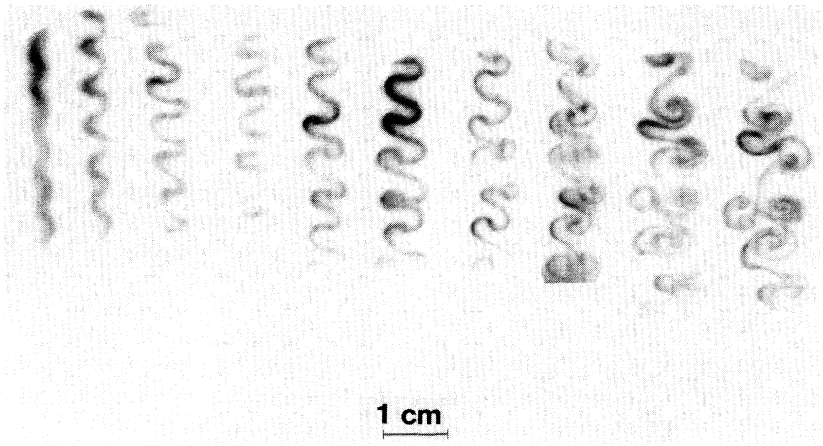

FIG. 4. Sinuous evolutions appear to lack vortex pairs until late times, and thereby mix the gases less effectively than mushroom profiles.

pulse time of our laser) show that flow of the SF_6/diacetyl layer remains stable for several seconds with only subtle variations. Also, we monitor the flow continuously with a schlieren system before each event. These PLIF and schlieren observations provide strong indirect evidence that initial conditions are reproducible, except for barely perceptible changes. Initial, shear-induced vorticity is much less than the shock-induced vorticity because the corresponding velocity changes are on the order of 100 times smaller. However, experimental limitations, (i.e., the availability of only one diagnostic laser) preclude direct correlation between initial conditions at the instant of shock impact and flow evolution.

Immediately after shock passage the three instability modes begin to evolve similarly. The perturbations on the upstream surfaces grow while the downstream perturbations invert, changing the initial varicose cross section into a thinner, sinuous one. The upstream mushroom shown in Fig. 2 develops cusps on the upstream edge and that edge grows slightly faster than the downstream edge. In Fig. 3 the layer evolves similarly, but in the opposite direction producing cusps facing downstream. In the sinuous-mode sequence, Fig. 4, each boundary grows at a comparable rate, thus retaining the symmetry of the sinuous shape and not showing cusps until much later than the mushroom modes. Mushroom profiles, Figs. 2 and 3, show prominent bumps and cusps that evolve into vortex pairs, creating the mushroom-shaped profile. Late in the process the mushrooms interact with neighboring vortex pairs, creating a more turbulent flow. In the late stages of the sinuous sequence, Fig. 4, vortices begin to appear but not in a coherent fashion. Growth amplitudes of the mushrooms are greater than those of the sinuous mode.

The initial behavior of a shock-accelerated layer can be qualitatively understood by considering the instability of each of the two boundaries of the layer independently. The linear RM instability predicts that perturbations on a light-heavy interface, i.e., the upstream interface, will grow linearly with time and without inversion. Disturbances on a heavy-light interface, i.e., the downstream boundary, will invert phase and then grow. Thus, the initial varicose profile of the perturbed gas layer shown in Fig. 5(a) is expected to evolve into a sinuous shape soon after shock impact.

The fluorescent images show clearly the presence of vortices in the mushroom modes, Figs. 2 and 3, and the absence of vortices in the sinuous mode (except at late time), Fig. 4. Vorticity is produced in these experiments by the misalignment of pressure and density gradients, sometimes referred to as baroclinic generation of vorticity. Because the dominant pressure gradient is produced by the plane shock wave, and the dominant density gradient is at the boundary of the gas layer [Fig. 5(a)], vorticity produced by the shock interaction will lie on the

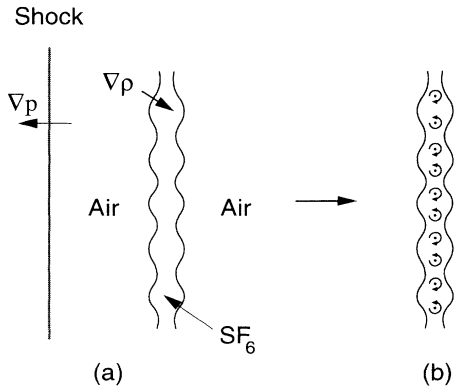

FIG. 5. Vorticity is generated by the interaction of the pressure gradient from a shock wave with the density gradient at the boundary of the layer (a). The resulting vorticity distribution can be roughly approximated as a row of equally spaced vortices (b).

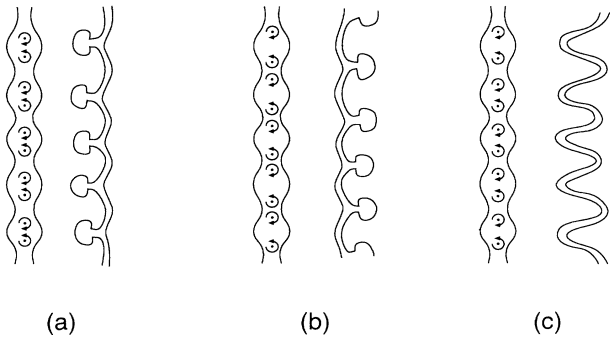

FIG. 6. The three patterns develop from slight differences in the initial vorticity distribution (shown greatly exaggerated). In (a) and (b) nonuniform vortex spacings cause vortices to pair producing mushroom-shaped features. A more equally spaced distribution develops into a sinuous shape as shown in (c). Counterclockwise and clockwise circulation is designated by circular arrows.

boundary of the layer, and will vary periodically along the layer. However, the boundary is diffuse and varies smoothly across the layer, and the layer is thin. Consequently, the shock interaction produces a vorticity distribution much like a row of diffuse, equally spaced vortices with alternating sign [Fig. 5(b)], rather than two sheets of vorticity.

A row of vortices is well known to be unstable [6]. One mode of instability can be generated by uniformly displacing every other vortex along the row, producing a row of vortex pairs. This vortex pairing causes the row of vortices to translate in a direction perpendicular to the row because the vortices induce motion inversely proportional to their separation. This mechanism produces a distribution of vortex pairs manifest as mushrooms moving upstream or downstream. Their orientation is shown schematically in Fig. 6. If the vortex spacing is smaller across the wider layer regions, Fig. 6(a), upstream mushrooms will form. Smaller vortex spacing across the narrower regions will produce downstream mushrooms, Fig. 6(b). Because the initial, shock-induced vorticity is actually distributed as blobs of vorticity, minute perturbations to the spacing may sufficiently damp the instability, producing distribution of unpaired vortices that we observe as the sinuous mode, Fig. 6(c). Thus the bifurcated flow can be qualitatively described by vorticity considerations. The absence of images with both upstream and downstream mushrooms (except at late times) suggests that the initial perturbation may systematically produce such a bias, or perhaps that some transverse wave correlates the disturbances.

In summary, the three distinct flow patterns of a shock-accelerated, thin, fluid layer that we observe are likely produced by subtle but important variations of the shock-induced vorticity at the RM unstable interfaces, and by the subsequent vortex dynamics. The bifurcated flow during the intermediate stage of RM instability growth produces well-ordered flow patterns, by contrast with disordered flow in the subsequent turbulence.

This research has been supported by U.S. Department of Energy Contract No. W-7405-ENG-36. We are grateful to R. Reinovsky and J. Shaner for advice and encouragement, to R. Haight for use of the camera, and to C. Findley and D. Bannerman for technical assistance.

[a]Present address: Physics Department, University of California, Berkeley, CA 94720.
[b]Present address: Physics Department, University of Chicago, Chicago, IL 60637.

[1] R. D. Richtmyer, Commun. Pure Appl. Math. **13**, 297–319 (1960).
[2] E. E. Meshkov, Izv. Akad. Nauk. SSSR Mekh. Zhidk. Gaza **4**, 151–157 (1969) [Fluid Dyn. **4**, 101–104 (1969)].
[3] Recent studies of the Richtmyer-Meshkov instability and references to earlier work are compiled in the Proceedings of the Physics of Compressible Turbulent Mixing Workshops: Advances in Compressible Turbulent Mixing, {*Proceedings of the First International Workshop on the Physics of Compressible Turbulent Mixing, Princeton, October 1988*, edited by W. P. Dannevik, A. C. Buckingham, and C. E. Leith (Lawrence Livermore Laboratory Report No. CONF-8810234, 1992); *Proceedings of the Third International Workshop on the Physics of Compressible Turbulent Mixing, Abbey of Royaumont, France, 17–19 June, 1991* [Commissariat à l'Energie Atomique (CEA) report]}.
[4] J. W. Jacobs, J. Fluid Mech. **234**, 629–649 (1992).
[5] A. H. Epstein, MIT Gas Turbine Laboratory Report No. 117, 1974 (unpublished).
[6] H. Lamb, *Hydrodynamics* (Dover, New York, 1945), p. 225, and references cited therein to von Kármán's studies.

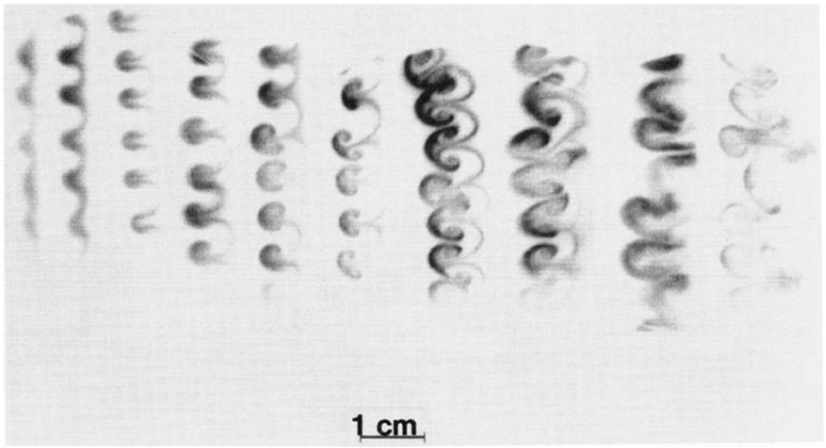

FIG. 2. This time sequence of PLIF images shows clearly one of the three distinct profiles that evolve from nearly identical initial conditions. Interframe time is about 100 μs. Because each image is taken on a different event, detailed features do not register frame to frame. However, the dominant growth features are reproducible. These "upstream mushrooms" have the mushroom caps oriented opposite to the direction of shock-wave motion. Darker regions indicate stronger fluorescent emission and therefore higher concentration of SF_6/diacetyl.

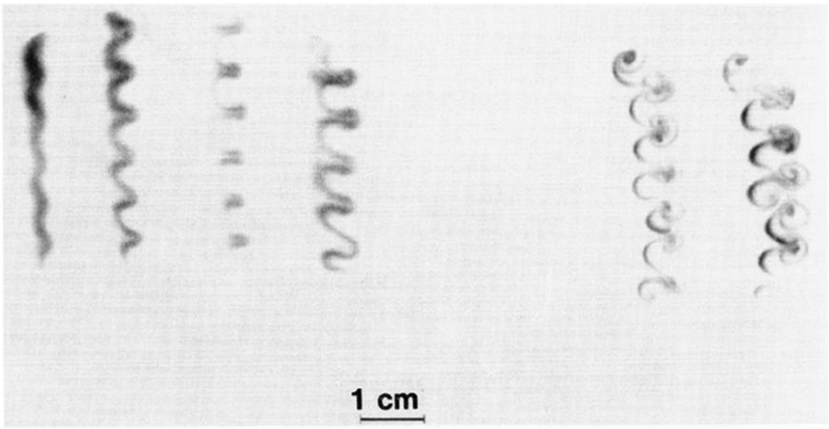

FIG. 3. The "downstream mushrooms" are similar to the upstream mushrooms but oppositely directed. They occur rarely in our experiments. Like upstream mushrooms, they appear to be driven by vortex pairs and produce mixing by entraining the ambient air within the SF_6 test gas.

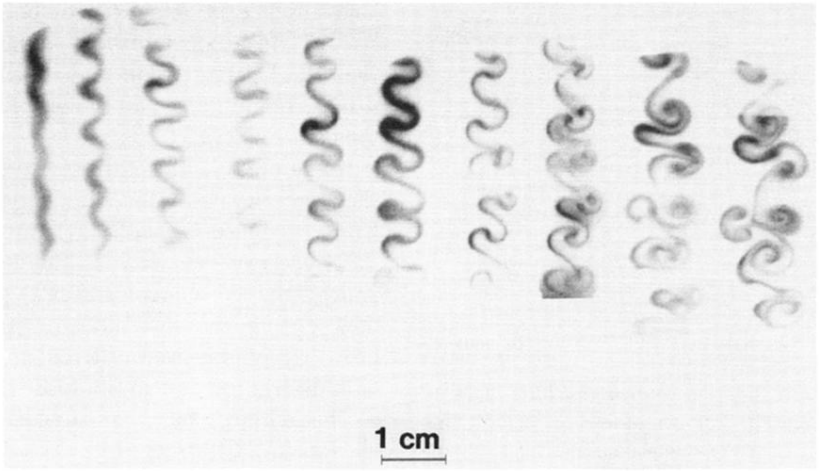

FIG. 4. Sinuous evolutions appear to lack vortex pairs until late times, and thereby mix the gases less effectively than mushroom profiles.